

Depth profiling in amorphous and microcrystalline silicon by transient photoconductivity techniques

This article has been downloaded from IOPscience. Please scroll down to see the full text article.

2002 J. Phys.: Condens. Matter 14 6909

(<http://iopscience.iop.org/0953-8984/14/28/302>)

View [the table of contents for this issue](#), or go to the [journal homepage](#) for more

Download details:

IP Address: 171.66.16.96

The article was downloaded on 18/05/2010 at 12:15

Please note that [terms and conditions apply](#).

Depth profiling in amorphous and microcrystalline silicon by transient photoconductivity techniques

R Brüggemann^{1,3}, C Main² and S Reynolds²

¹ Fachbereich Physik, Carl von Ossietzky Universität Oldenburg, D-26111 Oldenburg, Germany

² School of Science and Engineering, University of Abertay Dundee, Dundee DD1 1HG, UK

E-mail: rudi.brueggemann@uni-oldenburg.de

Received 14 March 2002

Published 5 July 2002

Online at stacks.iop.org/JPhysCM/14/6909

Abstract

We probe near-surface regions in hydrogenated amorphous and microcrystalline silicon by recording the transient photocurrent after application of a green laser pulse with short absorption depth through the glass-substrate/silicon interface. Depending on the spatial defect inhomogeneity close to the illuminated surface the transient photocurrent shows a different decay behaviour under strongly absorbed green light as compared with more uniformly absorbed red illumination. We apply a Fourier transform technique to the photocurrent decay, which reveals spatial inhomogeneities in the deep-defect density in amorphous silicon. For a highly crystalline sample of microcrystalline silicon we find depth homogeneity in the electronic properties, in agreement with information from structural investigations.

1. Introduction

Hydrogenated amorphous (a-Si:H) and microcrystalline (μ c-Si:H) silicon are semiconductors with interesting opto-electronic properties. They can be deposited at low substrate temperatures on inexpensive substrates such as glass, in plasma-enhanced chemical vapour deposition (PECVD) and hot-wire chemical vapour deposition (HWCVD) systems. Films grow typically between a few hundred and a several tens of thousands of ångströms thick. Knowledge and control of the defect density is important as recombination and thus the photoelectronic properties are determined by the dangling bond density in a-Si:H. The ability to distinguish between near-free surface, near-substrate interface and bulk defects is important because the electronic properties, for example in thin-film transistors, may be largely influenced by near-surface/interface states. Depth inhomogeneity in the deep-defect density and a deleterious influence of near-surface or interface states in a-Si:H have been reported by a number of authors [1–5].

³ Author to whom any correspondence should be addressed.

The situation in microcrystalline silicon is somewhat different, where, depending on the deposition conditions, the structural properties may change during film growth from amorphous to crystalline [6–8]. Deposition with no initial amorphous phase can also be achieved. It is clear that the electronic properties may change with depth if the growth behaviour changes drastically. An experimental technique for the identification of depth inhomogeneities, also influencing the electronic properties in the thin-film samples, would thus be useful.

In this paper, we present the application of transient photoconductivity (TPC), which measures the transient photocurrent following pulsed-light excitation, to reveal depth inhomogeneities: related to changes in the density-of-states (DOS) distribution in a-Si:H and to possible changes in the crystalline volume fraction in μ c-Si:H. Varying the wavelength and hence the absorption depth of the exciting laser light, and changing the side from which it is incident, allows us to probe the region close to the free surface, the substrate interface or the bulk of the sample.

2. Experimental details

2.1. Transient photoconductivity technique

In the computer-controlled TPC measurement system [9] a Gould 4072 digital storage oscilloscope records the transient photocurrent produced by a 4 ns light pulse from a Laser Science VSL337 dye laser. The overall current-decay data are assembled by piecing together several data sets, obtained by averaging a number of traces over a given time range and gain setting.

TPC yields information on the energetic profile $g(E)$ of the DOS in the context of a multi-trapping model by appropriate analysis of the time-dependent photocurrent $I_{\text{ph}}(t)$. Information is contained in $I_{\text{ph}}(t)$ on the trapping and release kinetics of excess charge carriers in localized gap-states, and hence on the DOS function $g(E)$. Fourier [10, 11] and Laplace [12–15] transform techniques allow the conversion of the photocurrent data into a DOS distribution over a wide energy range. Modulated photoconductivity (MPC) [16, 17] is complementary for determining the DOS distribution.

In this work, we apply a Fourier transform technique to the TPC results as originally described by Main *et al* [10] and subsequently applied [18, 19] for converting the photocurrent data into $g(E)$. The DOS at an energy E below the transport path is computed from the amplitude $\tilde{I}(\omega)$ and phase $\Phi(\omega)$ of the Fourier-transformed current transient according to

$$\frac{\nu}{N_c \mu} g(E) \propto \frac{\sin(\omega)}{\tilde{I}(\omega)}, \quad (1)$$

where ν is the attempt-to-escape frequency, μ the mobility of the conducting carriers and N_c the effective density of states in the transport band. The energy scale is given by $E = kT \ln(\nu/\omega)$, where k is Boltzmann's constant, T is the temperature and the angular frequency ω is the variable in the Fourier domain.

2.2. Sample details

We studied several samples from different deposition systems for which the deposition parameters had been adjusted to produce either amorphous or microcrystalline silicon. All samples were deposited on Corning 7059 glass. Coplanar aluminium contacts with 0.05 cm gap and 0.5 cm wide were deposited onto the films.

We studied a standard PECVD a-Si:H sample from Institut für Physikalische Elektronik (*ipe*), Universität Stuttgart. Another HWCVD a-Si:H sample was selected, which was deposited under non-optimized conditions when parametrizing the deposition conditions of

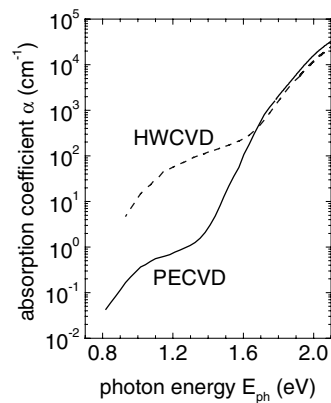


Figure 1. Comparison of the CPM-derived absorption coefficient between the PECVD and non-optimized HWCVD a-Si:H sample. The dangling-bond-related absorption is large and masks the Urbach tail in the HWCVD results. The data were calibrated against the absolute optical absorption coefficient.

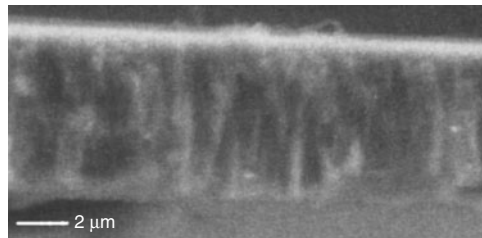


Figure 2. Scanning electron microscopy shows the columnar structure of the highly crystalline μ c-Si sample. The substrate is at the top of the figure.

a newly built HWCVD ultra-high-vacuum system at *ipe*. Figure 1 shows the absorption coefficient α from the constant-photocurrent method (CPM) [20] for the two samples, clearly indicating a much higher defect density in the HWCVD sample, deduced from the large sub-gap absorption coefficient. Note that the HWCVD sample also has a much higher absorption in the Urbach-tail region, in which α increases exponentially for the PECVD sample, indicating that dangling-bond-related absorption in the HWCVD sample is high and masks the Urbach tail.

A 4.4 μ m thick microcrystalline silicon sample from *ipe*, also deposited by HWCVD, was used for studying any depth inhomogeneity in a highly crystalline sample. Raman spectroscopy revealed a high crystalline volume fraction. Figure 2 shows a scanning electron microscope photograph with the columnar structure of the sample, typical for highly crystalline material. More information can be found elsewhere [21]. Electron-spin resonance showed a dangling bond defect density of the order of 10^{17} cm^{-3} [22].

In order to be sensitive to the spatial region close to the silicon/glass interface laser excitation in the green spectral range at 510 nm was used. The corresponding absorption depth d , taken as the inverse of the absorption coefficient, $d = 1/\alpha$, is between 0.08 and 0.09 μ m in the amorphous samples and about 0.3 μ m in the microcrystalline sample. In comparison, sample illumination with red laser light at 640 nm resulted in a fairly homogeneous photogeneration profile of excess carriers with an absorption depth of about 1.5 μ m in the amorphous samples and 3.1 μ m in the microcrystalline sample.

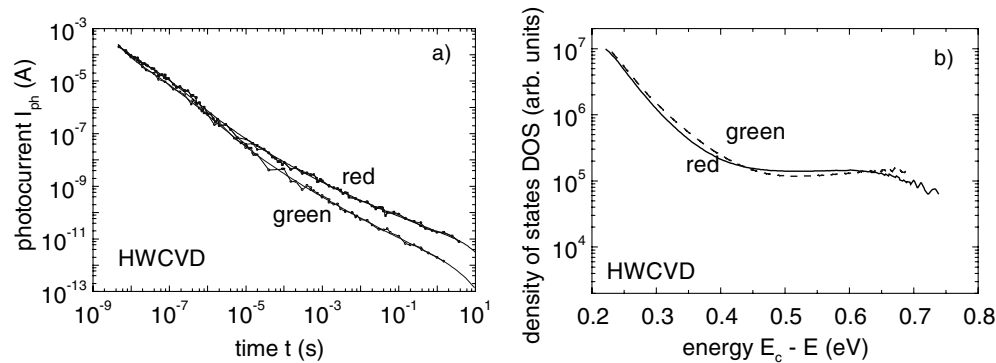


Figure 3. The transient photocurrent (a) and DOS profile (b) for the HWCVD sample. The conduction-band tail is slightly broader for the green illumination as reflected by the less steep photocurrent decay. The value for E_0 is about 40 meV.

3. Results

The results are organized into separate figures for each sample, presenting the photocurrent results taken at 300 K and the calculated DOS profile, respectively. Figure 3 shows for the HWCVD a-Si:H sample that green illumination from the substrate side and red illumination from the substrate side result in similar decay behaviour. Accordingly, the DOS profile is similar. The conduction-band tail in this non-optimized sample is exponential following $\exp[-(E_c - E)/E_0]$ with E_0 of 40 meV, larger than for standard a-Si:H.

Similar results as in figure 3 with no difference between bulk and surface regions have also been found for high-defect a-Si:H samples from other deposition techniques such as very-high-frequency PECVD.

Figure 4 shows for the PECVD a-Si:H sample of figure 1 that the difference in green illumination from the substrate and red illumination can be significant. For green illumination the current drops much faster at around 10^{-6} s, a feature much less pronounced for red illumination. The corresponding DOS profile shows that the larger deep defect density is responsible for the steeper decay. The band-tail parameter E_0 here is 30 meV in the bulk, not untypical for E_0 values from TPC at room temperature.

In figure 4(b), we have also included the DOS probed with light incident from the air/film interface. This also shows larger values when compared with the bulk, indicating a higher defect density at this interface.

Compared with the a-Si:H results, figure 5 for the μ c-Si:H sample shows a different decay behaviour. Apart from the slightly larger values for red illumination, no significant difference is seen in the evolution with time for green or red illumination. The DOS profile shows a broad decay, similar for the region close to the substrate and for the bulk.

4. Discussion

The TPC results for the two amorphous silicon samples can be discussed in the light of the much higher sub-gap absorption for the HWCVD a-Si:H sample shown in figure 1. For homogeneous illumination, the TPC-derived DOS for the HWCVD sample is larger, the conduction-band tail is broader and the dangling-bond-related shoulder at energies larger than about 0.4 eV below E_c is at a higher value. A fast TPC decay already at shorter times is seen for the HWCVD

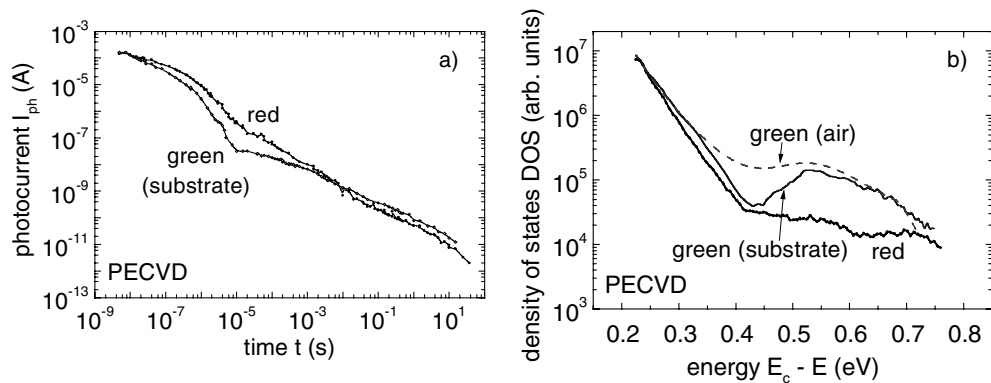


Figure 4. The transient photocurrent (a) and DOS profile (b) for the PECVD sample. In the near-substrate DOS there is a change in slope at around 0.32 eV. The deep-defect DOS near the surfaces, deduced from the green-light TPC, is larger than the red-light TPC bulk DOS. The bulk value for E_0 is about 30 meV.

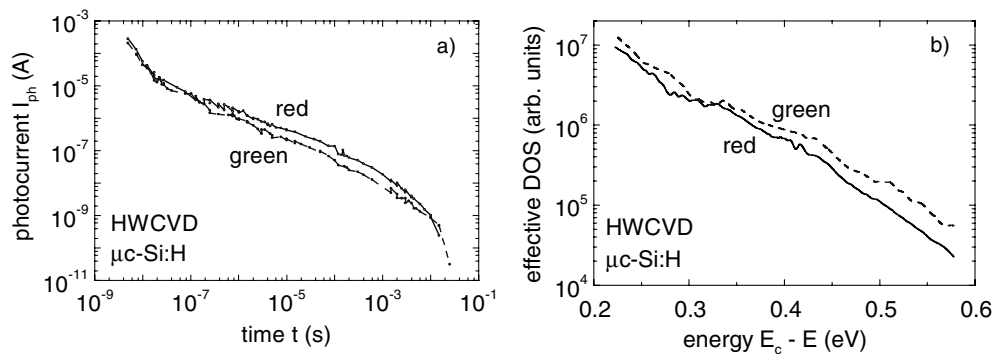


Figure 5. The transient photocurrent (a) and DOS profile (b) for the μc -Si HWCVD sample. The photocurrent decay is similar for the two illumination conditions leading to a similar DOS profile close to the substrate and in the bulk. The shape of the DOS is also different to that of standard a-Si:H. The ordinate label is an effective DOS as we expect that localized states are inhomogeneously distributed on a microscopic scale.

sample in figure 3(a), for both red and green illumination, indicating the high deep-trapping probability.

The lower dangling-bond density in the PECVD sample leads to a TPC decay for red illumination (figure 4) that falls somewhat more slowly up to a few times 10^{-7} s before deep trapping leads to a faster decay. The comparison with the TPC decay for green illumination in figure 4 indicates that within the smaller absorption depth close to the substrate interface a larger dangling-bond density is probed, leading to the faster decay at shorter times, followed by equilibration and thermal release from the dangling bond states.

The DOS results in figures 3 and 4 indicate that the TPC technique can be applied for depth profiling of the density of states. The HWCVD a-Si:H sample has been shown to have a homogeneous DOS with a large deep-defect density and a broad conduction-band tail with 40 meV characteristic tail slope.

For the PECVD a-Si:H samples further inferences may be made. In agreement with earlier reports [1, 2, 23], we find an increase in the deep-defect DOS, related to the dangling-

bond density close to the air/film interface and also close to the film/substrate interface. The DOS probed within the absorption depth close to the air/film interface has a slightly broader conduction-band tail as compared with the bulk. For the DOS close to the film/substrate interface a closer inspection shows a change in slope at around 0.32 eV. A feature appearing in this energy range was also found using the MPC technique [5] with green and red illumination, and was tentatively assigned to surface states close to the substrate interface. Improved resolution of this feature could be achieved by performing TPC at lower temperature to reduce thermal broadening in the TPC-DOS [9].

The TPC results for the microcrystalline sample, shown in figure 5, do not differ qualitatively for red and green illumination. They are similar to the results previously reported for microcrystalline silicon deposited in a different deposition system [24]. The two DOS profiles are similar, indicating that the sample is quite homogeneous with respect to its electronic properties, which are determined to a large degree by the underlying DOS distribution.

It is interesting to note that spectral photoluminescence (PL) of this $\mu\text{c-Si:H}$ sample with green-light excitation through the glass gives no hint of an amorphous layer [25], which is consistent with our TPC results. Given the spatial sensitivity demonstrated for the amorphous silicon PECVD sample, it should be possible to detect the initial amorphous growth region in $\mu\text{c-Si}$ with the TPC technique described here. Of course, for complete covering of the near-substrate region and to monitor the evolution from amorphous to microcrystalline growth, TPC with shorter wavelength to achieve smaller absorption depths is necessary for $\mu\text{c-Si:H}$.

We believe the technique will be useful for studying the influence of depth inhomogeneities in thin-film semiconductors, important for example in a-Si:H or $\mu\text{c-Si:H}$ layers for thin-film transistors with different materials used as substrates. In contrast, sub-gap absorption using the standard CPM fails to be near-surface/surface sensitive [26] to deep defects. TPC not only determines the density of deep defects but also provides the energetic resolution of the DOS distribution.

5. Conclusion

We have shown that TPC is sensitive to the absorption depth of the exciting light and that the changes in photocurrent decay may be correlated with changes in defect density associated with structural inhomogeneities. In amorphous silicon the technique identifies defective layers and spatial variations of the DOS distribution. For microcrystalline silicon we showed that highly crystalline $\mu\text{c-Si:H}$ has homogeneous electronic properties. Variation of the wavelength and corresponding material-related variation of the absorption depth offer the potential for more detailed spatial profiling.

Acknowledgments

The authors thank A Hierzenberger and T Neidlinger, Institut für Physikalische Elektronik, Universität Stuttgart, for sample deposition. RB thanks the Deutsche Forschungsgemeinschaft, Bonn, for financial support. The authors also thank W Steidle, Institut für Physikalische Elektronik for taking the SEM photograph.

References

- [1] Hasegawa S and Imai Y 1982 *Phil. Mag.* **B 46** 239
- [2] Xu X, Morimoto A, Kumeda M and Shimizu T 1987 *Japan. J. Appl. Phys.* **26** L1818

- [3] Li Y M, Dawson R M, Collins R W and Wronski C R 1991 *Appl. Phys. Lett.* **59** 2549
- [4] Asano A and Stutzmann M 1991 *J. Appl. Phys.* **70** 5025
- [5] Kleider J P, Longeaud C and Roca i Cabarrocas P 1992 *J. Appl. Phys.* **72** 4727
- [6] Luysberg M, Hapke P, Carius R and Finger F 1997 *Phil. Mag. A* **75** 31
- [7] Vallat-Sauvain E, Kroll U, Meier J, Shah A and Pohl J 2000 *J. Appl. Phys.* **87** 3137
- [8] Finger F, Vetterl O, Carius R, Lambertz A, Scholten C, Houben L and Luysberg M 2001 *Materials for Information Technology in the New Millennium* ed J M Marshall, A G Petrov, A Vavrek, D Nesheva, D Dimova-Malinovska and J M Maud (Swansea: University of Wales) p 26
- [9] Reynolds S, Main C, Webb D P and Rose M J 2000 *Phil. Mag. B* **80** 547
- [10] Main C, Brüggemann R, Webb D P and Reynolds S 1992 *Solid State Commun.* **83** 401
- [11] Main C 1997 *MRS Symp. Proc.* **467** 167
- [12] Naito H and Okuda M 1995 *J. Appl. Phys.* **77** 3541
- [13] Nagase T, Kishimoto K and Naito H 1999 *J. Appl. Phys.* **86** 5026
- [14] Ogawa N, Nagase T and Naito H 2000 *J. Non-Cryst. Solids.* **266** 367
- [15] Gueorguieva M J, Main C and Reynolds S 2000 *MRS Symp. Proc.* **609** A27.8
available at <http://www.mrs.org/publications/epubs/proceedings/spring2000/a/>.
- [16] Brüggemann R, Main C, Berkin J and Reynolds S 1990 *Phil. Mag. B* **62** 29
- [17] Kleider J P and Longeaud C 1995 *Solid State Phenom.* **44–46** 597
- [18] Webb D P, Main C, Brüggemann R and Reynolds S 1994 *Proc. 12th Eur. Photovoltaic Solar Energy Conf. (Amsterdam)* ed R Hill, W Palz and P Helm (Bedford: Stephens) p 124
- [19] Main C, Brüggemann R, Webb D P and Reynolds S 1994 *J. Non-Cryst. Solids* **164** 481
- [20] Vaneček M, Kočka J, Stuchlik J and Triska A 1981 *Solid State Commun.* **39** 1199
- [21] Brüggemann R, Hierzenberger A, Reinig P, Rojahn M, Schubert M B, Schweizer S, Wanka H N and Zrinčzak I 1998 *J. Non-Cryst. Solids* **227–230** 982
- [22] Kanschat P, Lips K, Brüggemann R, Hierzenberger A, Sieber I and Fuhs W 1998 *MRS Symp. Proc.* **507** 793
- [23] Kleider J P, Longeaud C and Glodt O 1991 *J. Non-Cryst. Solids* **137/138** 447
- [24] Brüggemann R, Kleider J P, Longeaud C, Mencaraglia D, Guillet J, Bouree J E and Niikura C 2000 *J. Non-Cryst. Solids* **266** 258
- [25] Klein S 2002 private communication
PL measurements were performed at Institut für Physikalische Elektronik, Universität Stuttgart
- [26] Amato G, Benedetto G, Boarino L and Spagnolo R 1991 *Solid State Commun.* **77** 177